

Biophysical Journal, Volume 112

Supplemental Information

Role of Pore-Lining Residues in Defining the Rate of Water Conduction

by Aquaporin-0

Patrick O. Saboe, Chiara Rapisarda, Shreyas Kaptan, Yu-Shan Hsiao, Samantha R. Summers, Rita De Zorzi, Danijela Dukovski, Jiaheng Yu, Bert L. de Groot, Manish Kumar, and Thomas Walz

Supplementary Information

**Role of pore-lining residues in defining the rate
of water conduction by aquaporin-0**

Table S1. Increase in water permeability of AQP0 proteoliposomes prepared with low lipid-to-protein ratios compared to pure lipid vesicles.

Lipid	LPR (mg/mg)	mLPR (mol/mol)	Factor increase in water permeability of AQP0 proteoliposomes over that of control vesicles
DMPC	2.0	78	3.5 ± 0.8
PC/PG 4:1 (mol/mol)	2.6	89	2.2 ± 0.8
<i>E. coli</i> polar lipids	2.4	78	2.2 ± 0.3

Table S2. Increase in water permeability of AQP0 proteoliposomes prepared with different lipid-to-protein ratios compared to pure lipid vesicles and the effect of cholesterol. Addition of cholesterol decreases the water leakage through the lipid bilayers, making it easier to measure the increase in water permeability due to AQP0.

Lipid	LPR (mg/mg)	mLPR (mol/mol)	Factor increase in water permeability of AQP0 proteoliposomes over that of control vesicles
	14.9	500	1.3 ± 0.7
PC/PG 4:1 (mol/mol)	2.6	89	2.2 ± 0.8
PC/PG/Chl 2:1:2 (mol/mol)	11.9	500	2.0 ± 0.5
	2.1	89	3.0 ± 0.9
PC/PS/Chl 4:1:5 (mol/mol)	11.2	500	1.5 ± 0.6
	2.0	89	3.8 ± 1.8

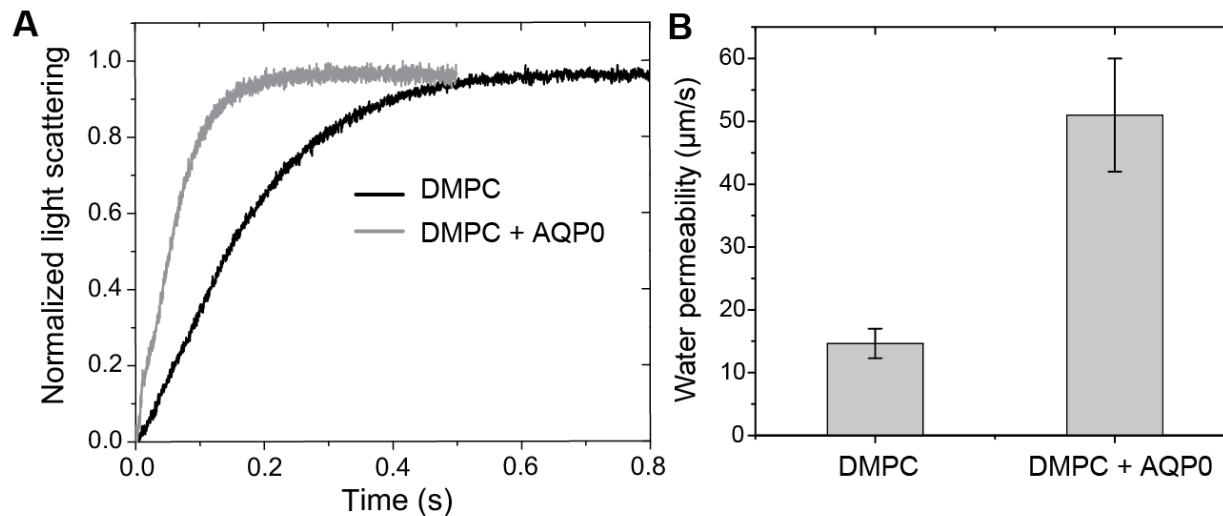


Figure S1. Water permeability of pure DMPC vesicles and AQP0-containing DMPC proteoliposomes. **A)** Stopped-flow light scattering traces obtained with pure DMPC vesicles (black trace) and AQP0 proteoliposomes resulting from reconstitution at an LPR of 2 (mg/mg; molar LPR of 78) (gray trace). **B)** The water permeability of pure DMPC vesicles at pH 6.5 was $14.7 \pm 2.3 \mu\text{m/s}$ and that of the AQP0 proteoliposomes was $51.0 \pm 9.0 \mu\text{m/s}$, corresponding to an increase by a factor of 3.5 ± 0.8 . The values are the average of three independent measurements and the error bars represent the standard deviation of the measurements. For DMPC, the experimental temperatures were adjusted to stay above the phase transition temperature of the lipid (37°C was used for dialysis and 25°C was used for stopped-flow measurements).

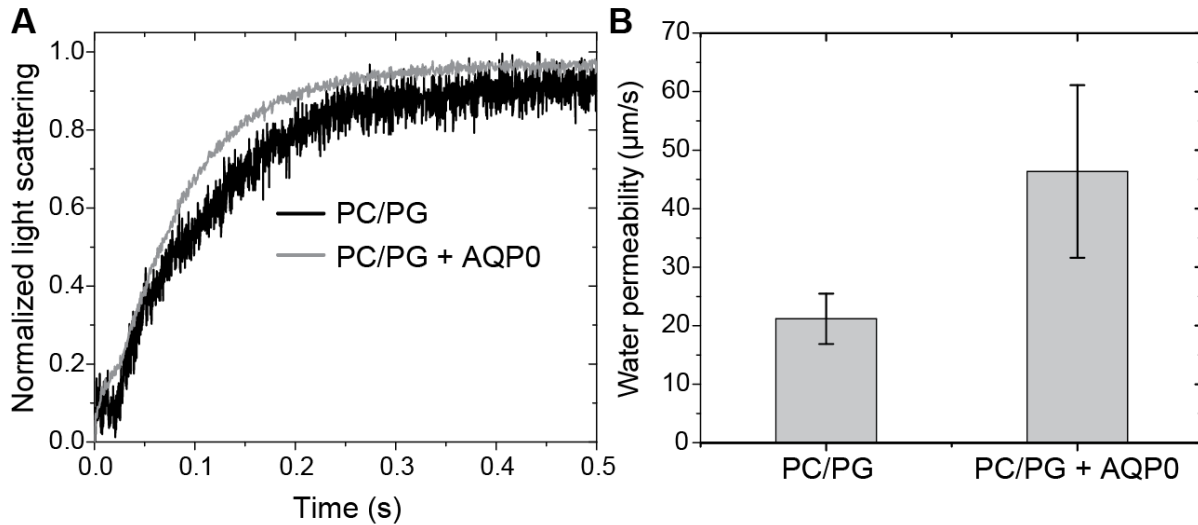


Figure S2. Water permeability of pure PC/PG (molar ratio of 4:1) vesicles and AQP0-containing PC/PG proteoliposomes. **A)** Stopped-flow light scattering traces obtained with pure PC/PG vesicles (black trace) and AQP0 proteoliposomes resulting from reconstitution at an LPR of 2.6 (mg/mg; molar LPR of 89) (gray trace). **B)** The water permeability of pure PC/PG vesicles at pH 6.5 was $21.2 \pm 4.3 \mu\text{m/s}$ and that of the AQP0 proteoliposomes was $46.4 \pm 14.8 \mu\text{m/s}$, corresponding to an increase by a factor of 2.2 ± 0.8 . The values are the average of three independent measurements and the error bars represent the standard deviation of the measurements.

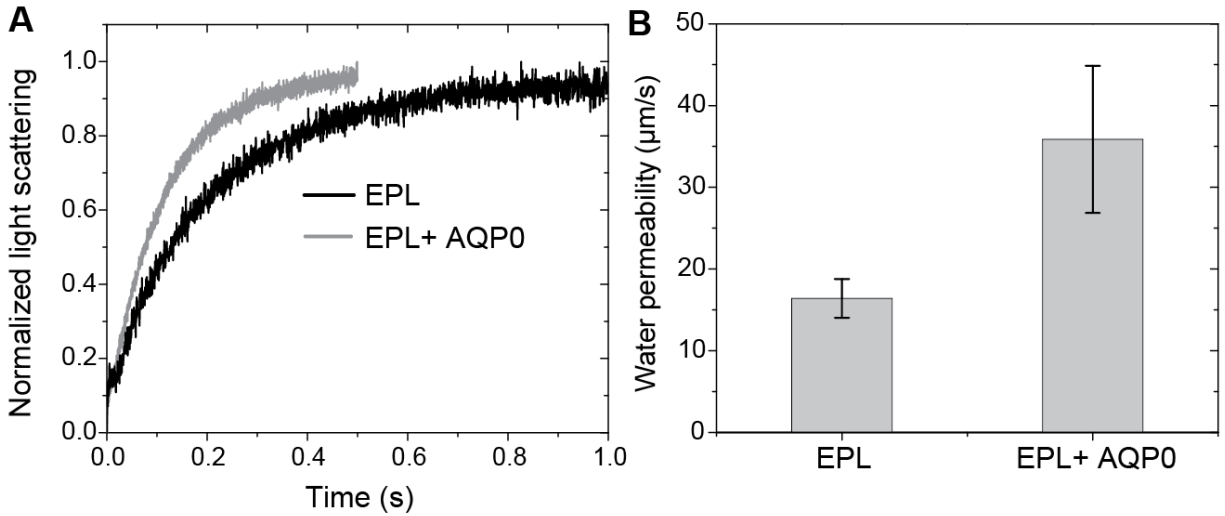


Figure S3. Water permeability of pure *E. coli* polar lipids (EPL) vesicles and AQP0-containing EPL proteoliposomes. **A)** Stopped-flow light scattering traces obtained with pure EPL vesicles (black trace) and AQP0 proteoliposomes resulting from reconstitution at an LPR of 2.4 (mg/mg; molar LPR of 78) (gray trace). **B)** The water permeability of pure EPL vesicles at pH 6.5 was $16.4 \pm 1.4 \mu\text{m/s}$ and that of the AQP0 proteoliposomes was $35.9 \pm 1.0 \mu\text{m/s}$, corresponding to an increase by a factor of 2.19 ± 0.2 . The values are the average of three independent measurements and the error bars represent the standard deviation of the measurements.

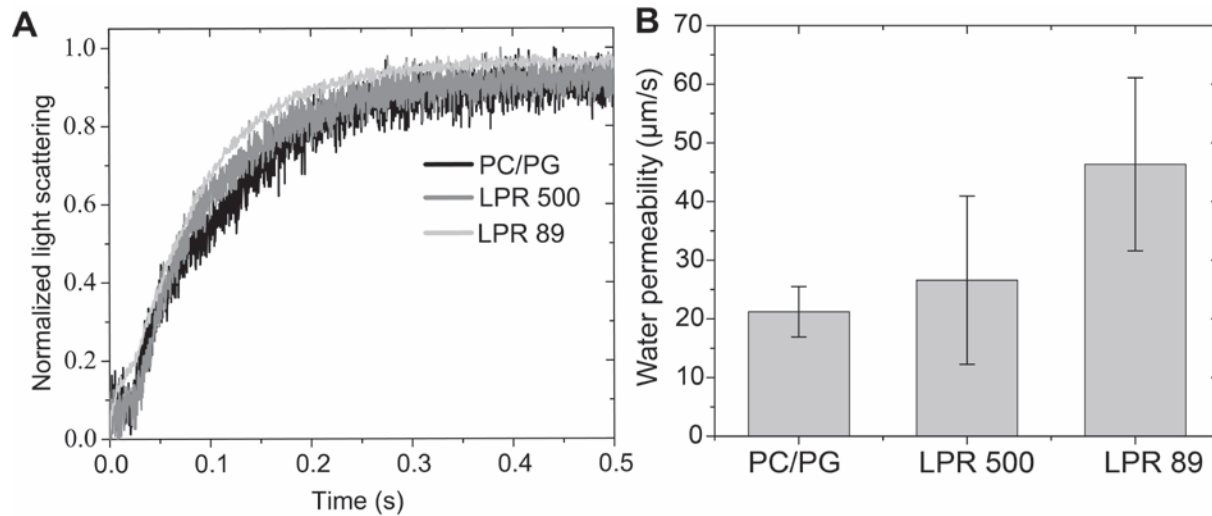


Figure S4. The water permeability of PC/PG (molar ratio of 4:1) vesicles is similar to those of AQP0-containing PC/PG proteoliposomes. **A**) Stopped-flow light scattering traces obtained with pure PC/PG vesicles (black trace) and AQP0-containing PC/PG proteoliposomes resulting from reconstitution at an LPR of 14.9 (mg/mg; molar LPR of 500) (dark gray trace) or at an LPR of 2.6 (mg/mg; molar LPR of 89) (light gray trace). Due to the low signal-to-noise ratio the three traces are poorly separated, but the noise level is reduced for proteoliposomes reconstituted at an LPR of 2.6. **B**) The water permeability of pure PC/PG vesicles at pH 6.5 was $21.4 \pm 4.3 \mu\text{m/s}$ and that of AQP0 proteoliposomes obtained with a molar LPR of 500 was $26.6 \pm 14.3 \mu\text{m/s}$, similar to that of the pure lipid vesicles. The water permeability of AQP0 proteoliposomes reconstituted at a molar LPR of 89 was $46.4 \pm 14.8 \mu\text{m/s}$, corresponding to an increase by a factor of 2.2 ± 0.8 over control liposomes. The values are the average of three independent measurements and the error bars represent the standard deviation of the measurements.

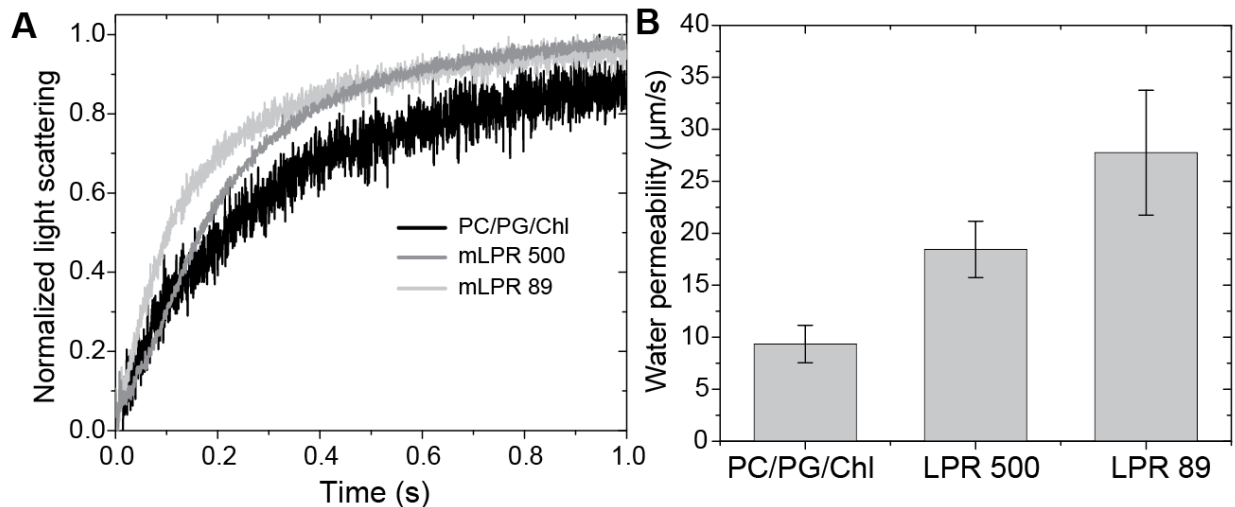


Figure S5. Cholesterol lowers the water permeability of PC/PG/Chl (molar ratio of 2:1:2) control vesicles, making it possible to clearly see the contribution of AQP0 to the water permeability of the vesicles. A) Stopped-flow light scattering traces obtained with PC/PG/Chl vesicles (black trace) and AQP0-containing PC:PG:Chl proteoliposomes resulting from reconstitution at an LPR of 11.9 (mg/mg; molar LPR of 500) (dark gray trace) or at an LPR of 2.1 (mg/mg; molar LPR of 89) (light gray trace). **B)** The water permeability of pure PC/PG/Chl vesicles at pH 6.5 was $9.3 \pm 1.8 \mu\text{m/s}$. The water permeabilities of AQP0 proteoliposomes reconstituted at molar LPRs of 500 and 89 were $18.4 \pm 2.7 \mu\text{m/s}$ and $27.8 \pm 6.0 \mu\text{m/s}$, respectively, corresponding to increases by factors of 2.0 ± 0.5 and 3.0 ± 0.9 over control liposomes. The values are the average of three independent measurements and the error bars represent the standard deviation of the measurements.

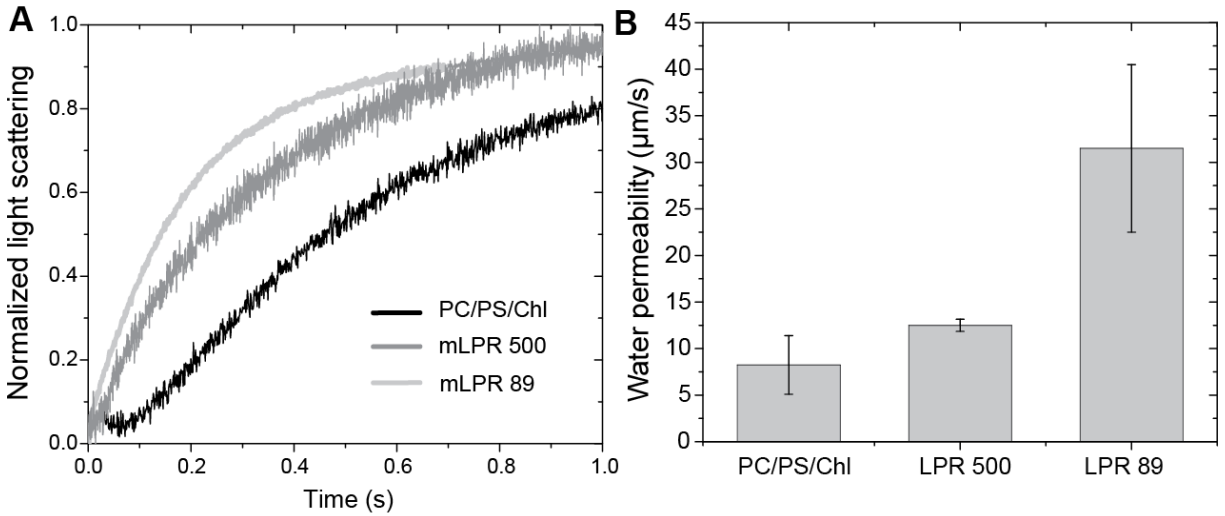


Figure S6. Cholesterol lowers the water permeability of PC:PS:Chl (molar ratio of 4:1:5) control vesicles, making it possible to clearly see the contribution of AQP0 to the water permeability of the vesicles. A) Stopped-flow light scattering traces obtained with PC/PS/Chl vesicles (black trace) and AQP0-containing PC/PS/Chl proteoliposomes resulting from reconstitution at an LPR of 11.2 (mg/mg; molar LPR of 500) (dark gray trace) or at an LPR of 2.0 (mg/mg; molar LPR of 89) (light gray trace). B) The water permeability of pure PC/PS/Chl vesicles at pH 6.5 was $8.25 \pm 3.2 \mu\text{m/s}$. The water permeabilities of AQP0 proteoliposomes reconstituted at molar LPRs of 500 and 89 were $12.5 \pm 0.7 \mu\text{m/s}$ and $31.6 \pm 8.9 \mu\text{m/s}$, respectively, corresponding to increases by factors of 1.5 ± 0.6 and 3.8 ± 1.8 over control liposomes. The values are the average of three independent measurements and the error bars represent the standard deviation of the measurements.

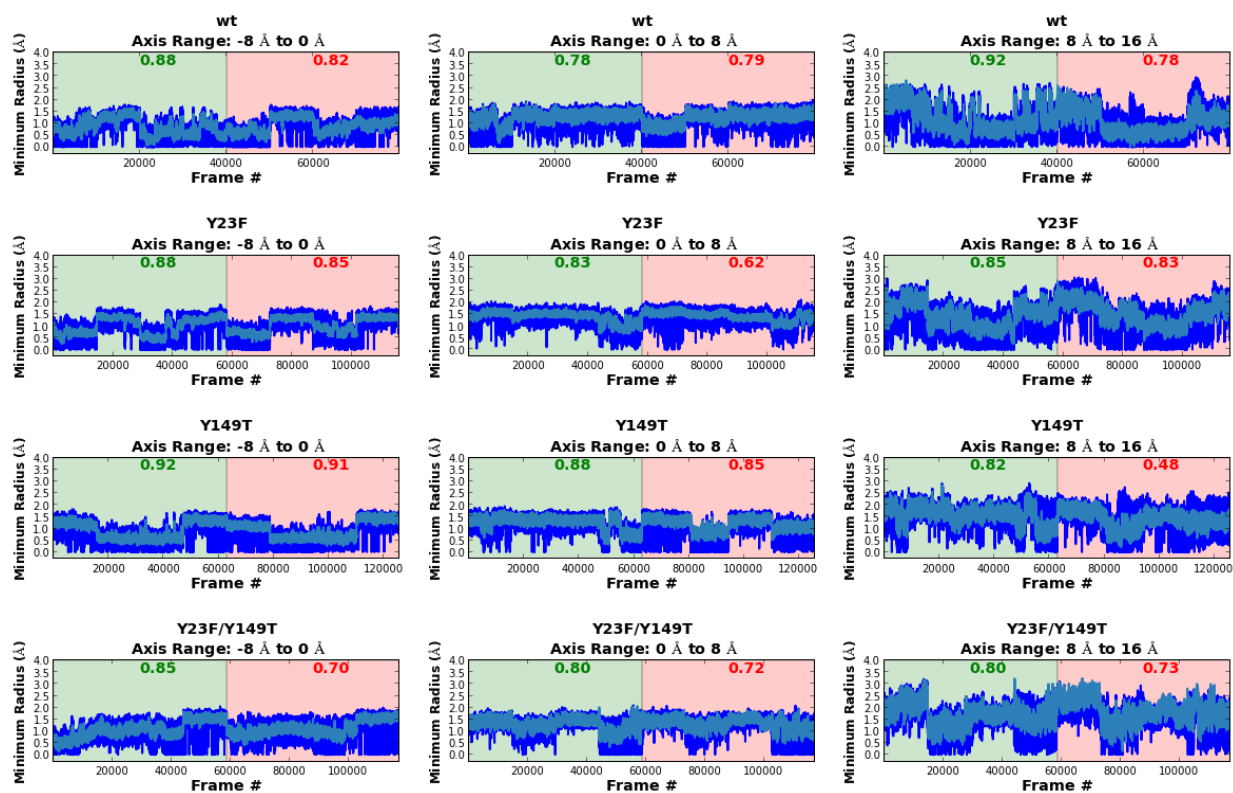


Figure S7. PLS-FMA analysis. Prediction of FMA modes from three sections of the monomer for wild-type AQP0 and the three tyrosine mutants. The training and validation regions are shown in light green and light red, respectively. The corresponding correlation coefficients are given in green and red bold font. The raw simulation data are shown in dark blue and the data modeled from PLS-FMA are shown in light blue.

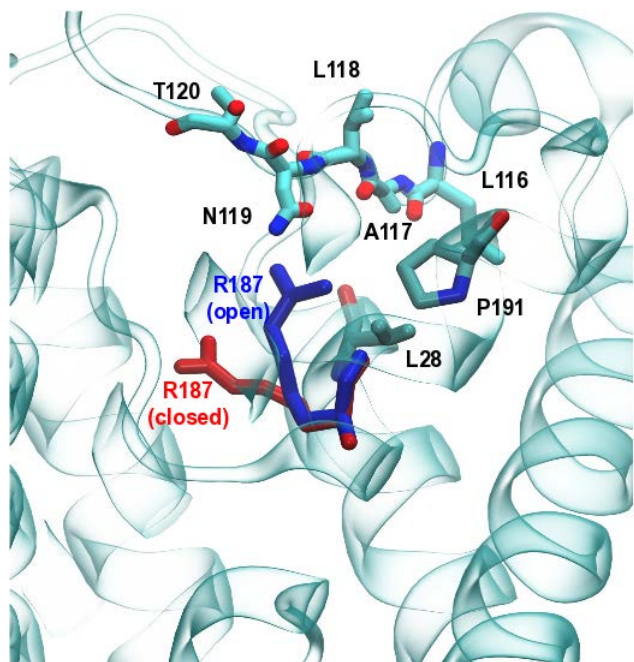


Figure S8. Mutations predicted to stabilize the arginine gate in the open state. The figure shows seven residues that are close to residue Arg-187. Mutations of these residues to either glutamate or aspartate are predicted to stabilize the arginine gate in the open state. These residues, except Pro-191 and Leu-28, are all on extracellular loop C of AQP0.

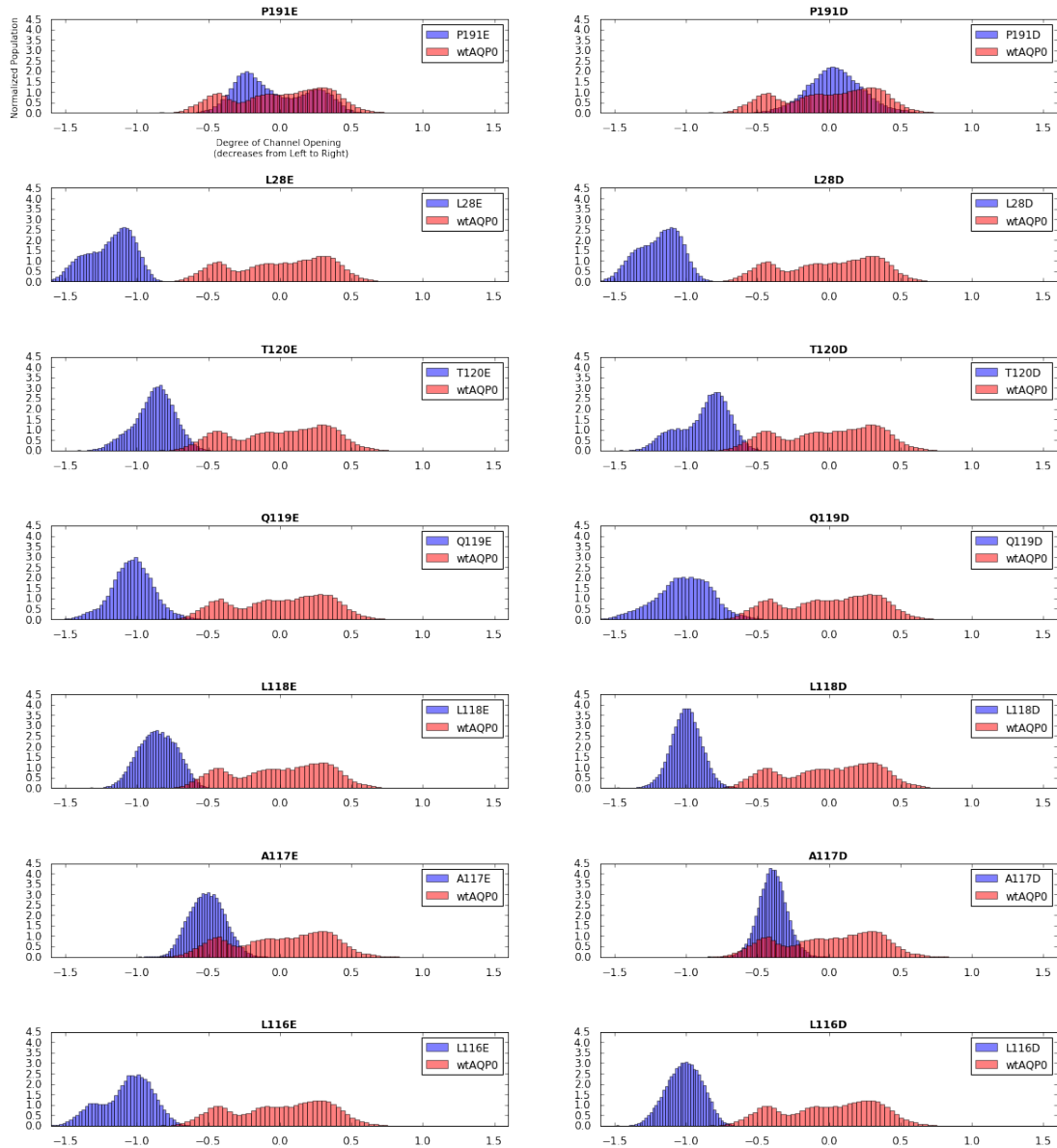


Figure S9. Population distributions of AQP0 proteins with mutations designed to keep the arginine gate in the open state. Except for mutations of Proline-191, the distribution of all investigated mutants is shifted to the right as compared to wild-type AQP0, confirming that the arginine mode remains in the “open” state. The same x-axis “degree of channel opening” applies to each panel.

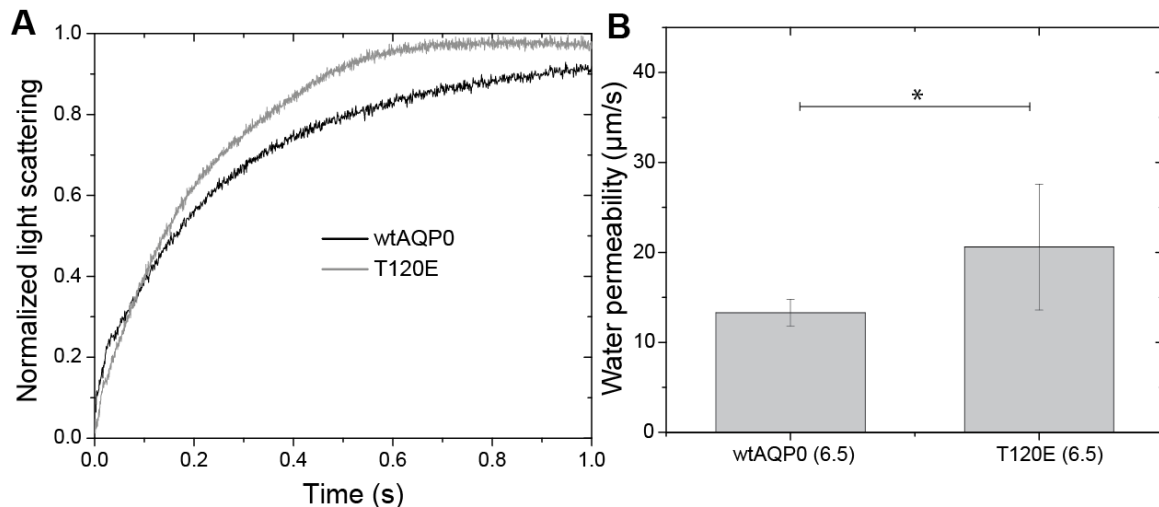


Figure S10. Water permeability of wild-type AQP0 and the T120E mutant reconstituted into PC/PS/Chl vesicles at an LPR 2.0. **A)** Stopped-flow light scattering traces obtained with wild-type AQP0 (black trace) and the T120E mutant (gray trace). **B)** The water permeability of pure wtAQP0 at pH 6.5 was $13.3 \pm 1.5 \mu\text{m/s}$ and that of the T120E mutant was $20.3 \pm 6.5 \mu\text{m/s}$. The values are the average of three independent measurements and the error bars represent the standard deviation of the measurements. ANOVA gives a p-value of 0.064, and there is ~93% confidence that the water permeability of the T120E mutant is different from that of wtAQP0.

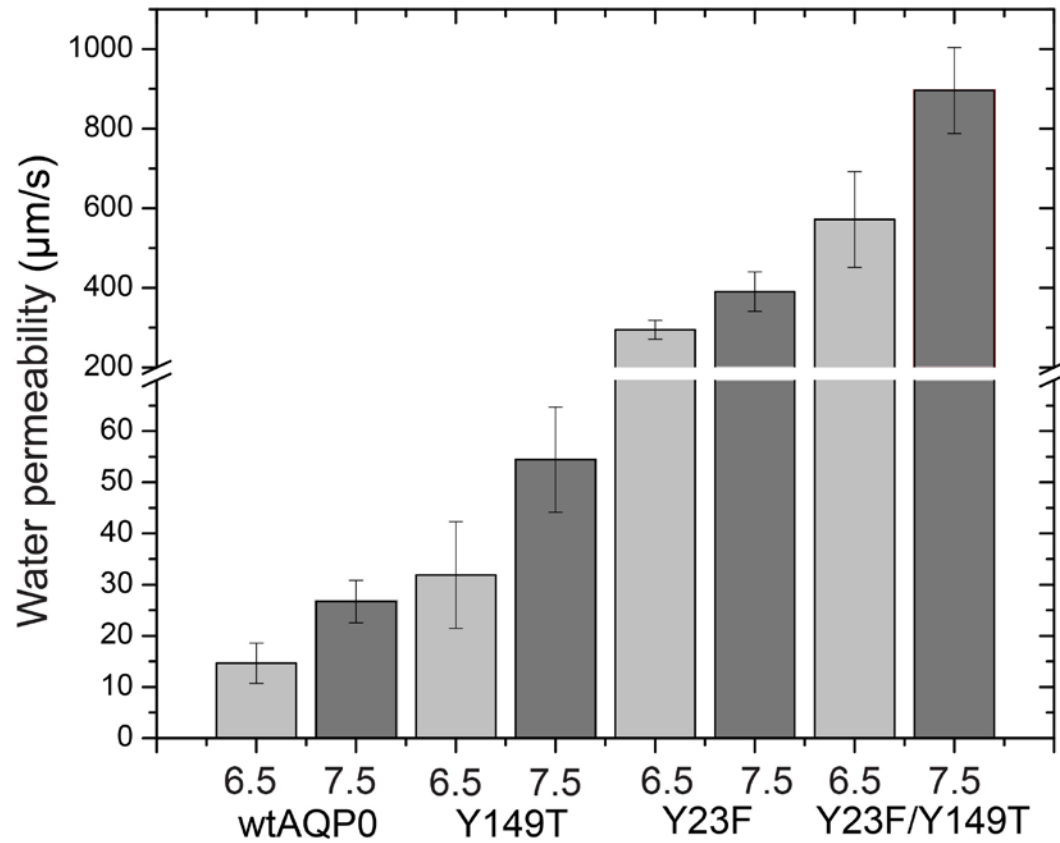


Figure S11. pH sensitivity of wild-type AQP0 and the tyrosine mutants. For wild-type AQP0 and for the Y23F, Y149T and Y23F/Y149T mutants, water permeability is slightly but consistently higher at pH 7.5 than at pH 6.5.

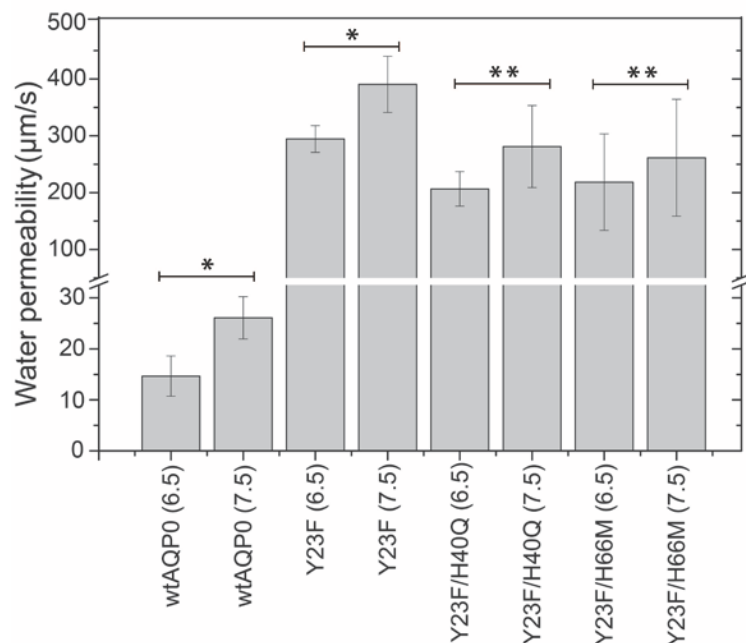


Figure S12. Water permeability at pH 6.5 and 7.5 of wild-type AQP0 and AQP0 mutants in which histidine residues were mutated. Proteoliposomes containing wild-type AQP0 and the Y23F mutant both show statistically significant higher water permeability at pH 7.5 than at pH 6.5 ($p < 0.05$), but differences in permeability were more readily resolved with the Y23F mutant. The water permeability of the H40Q/Y23F was $206.5 \pm 30.4 \mu\text{m/s}$ at pH 6.5 and $281 \pm 72 \mu\text{m/s}$ at pH 7.5, an increase by a factor of 1.4 ± 0.4 . The water permeability of the H66M/Y23F was $218.5 \pm 85 \mu\text{m/s}$ at pH 6.5 and $262 \pm 103 \mu\text{m/s}$ at pH 7.5, an increase by a factor of 1.2 ± 0.7 . Differences in water permeability at pH 6.5 and 7.5 of the Y23F/H40Q and Y23F/H66M double mutants were not statistically significant with a 95% confidence threshold ($p = 0.2$ for Y23F/H40Q and $p = 0.6$ for Y23F/H66M), suggesting that the two histidine residues may have a role in the subtle pH sensitivity of AQP0 water permeability. The error bars represent the standard deviation of the measurement. * $p < 0.05$, ** $p > 0.05$

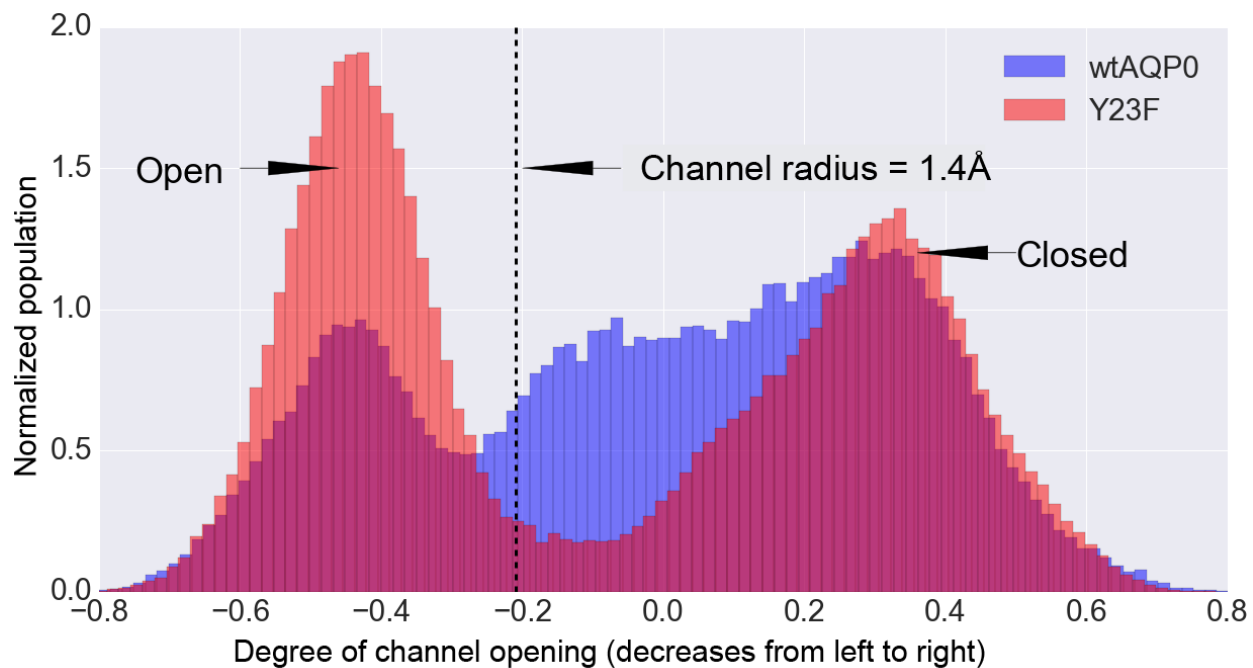


Figure S13. Population distributions along the PLS-FMA modes. Populations of wild-type AQP0 and the Y23F mutant along the arginine gate mode. The Y23F mutant spends almost twice as much time in the open state of the mode as the wild-type protein.

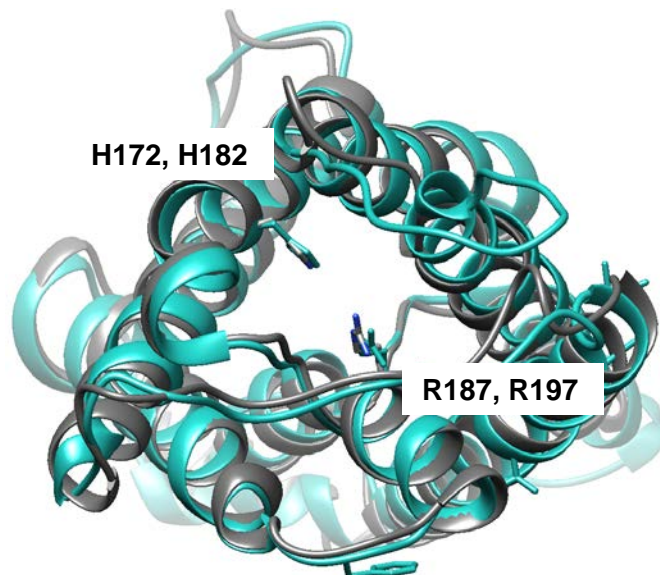


Figure S14. AQP1 (PDB id: 1J4N; light blue) has a histidine residue, His-182, that corresponds to His-172 in AQP0 (PDB id: 2B6O; gray, side chains of residues colored by element). Since AQP1 features a corresponding histidine residue but is not pH-sensitive, His-172 in AQP0 is unlikely to be involved in pH sensitivity. Furthermore, Arg-187 of AQP0 and Arg-197 of AQP1 are in close proximity to His-172 and His-182, respectively. The proximity of the arginine residues to the histidine residues likely shifts the pKa of the histidine residues beyond the physiological range.